Retinoblastoma Tumor Suppressor Gene Expression Determines the Response to Sequential Flavopiridol and Doxorubicin Treatment in Small-Cell Lung Carcinoma

Tulin Budak-Alpdogan,[1] Bobin Chen,[1,4] Anjali Warrier,[1] Daniel J. Medina,[1] Dirk Moore,[2] and Joseph R. Bertino[1,3]

Abstract

Purpose: Small-cell lung cancers (SCLC) are defective in many regulatory mechanisms that control cell cycle progression, i.e., functional retinoblastoma protein (pRb). Flavopiridol inhibits proliferation and induces apoptosis in SCLC cell lines. We hypothesized that the sequence flavopiridol followed by doxorubicin would be synergistic in pRb-deficient SCLC cells.

Experimental Design: A H69 pRb-deficient SCLC cell line, H865, with functional pRb and H865 pRb small interfering RNA (siRNA) knockdown cells were used for *in vitro* and *in vivo* experiments. The *in vivo* efficiencies of various sequential combinations were tested using *nude*/*nude* athymic mice and human SCLC xenograft models.

Results: Flavopiridol then doxorubicin sequential treatment was synergistic in the pRB-negative H69 cell line. By knocking down pRb with specific siRNA, H865 clones with complete pRb knockdown became sensitive to flavopiridol and doxorubicin combinations. pRb-deficient SCLC cell lines were highly sensitive to flavopiridol-induced apoptosis. pRb-positive H865 cells arrested in G_0-G_1 with flavopiridol exposure, whereas doxorubicin and all flavopiridol/doxorubicin combinations caused a G_2-M block. In contrast, pRb-negative SCLC cells did not arrest in G_0-G_1 with flavopiridol exposure. Flavopiridol treatment alone did not have an *in vivo* antitumor effect, but sequential flavopiridol followed by doxorubicin treatment provided tumor growth control and a survival advantage in Rb-negative xenograft models, compared with the other sequential treatments.

Conclusions: Flavopiridol and doxorubicin sequential treatment induces potent *in vitro* and *in vivo* synergism in pRb-negative SCLC cells and should be clinically tested in tumors lacking functional pRB.

Small-cell lung cancer (SCLC) accounts for ~13% of the lung cancers (1, 2). Despite the high response rate of SCLC to many anticancer agents, during the last 30 years there has been only a modest change in survival, particularly for patients with extensive-stage disease. Although the initial complete response rate is ~80% in extensive-stage disease, the commonly used regimens have achieved a median survival of less than 12 months (2, 3). Comparative trials have shown that multidrug regimens, alternating agents, or dose-dense high-dose regimens are no better than cisplatin plus etoposide, a standard two-drug regimen (2, 4–6). An understanding of the molecular pathogenesis of SCLC may lead to new treatment strategies.

The retinoblastoma (pRb) tumor suppressor gene is inactivated in more than 90% of SCLC (7, 8) and, consequently, is the most common molecular abnormality in SCLC. pRb has a critical role in the proliferative response of the cells to mitogenic signals (9–11). Phosphorylation of the Rb protein is regulated in a cell cycle–dependent manner. Hypophosphorylated Rb protein assembles transcriptional repressor complexes on promoters of E2F-regulated genes and inhibits cell cycle progression. Cells respond to mitogenic signals by sequential activity of cyclin–cyclin-dependent kinase complexes and phosphorylation of pRb. This chain of events disrupts the Rb interaction with E2F1-3 family members and releases the cells into cell cycle progression. Thus, pRb is considered to be the master regulator of the G_1-S phase transition (9–11).

Doxorubicin, a widely used chemotherapeutic for SCLC, has cytotoxic activity in all phases of the cell cycle, more predominantly during the S phase. The aromatic chromophore portion of doxorubicin interacts with two base pairs of the DNA by intercalation (12, 13). This inhibits the progression of the

Authors' Affiliations: Departments of [1]Medicine and [2]Biometrics, University of Medicine and Dentistry of New Jersey-Robert Wood Johnson Medical School, Cancer Institute of New Jersey; [3]Department of Pharmacology, Robert Wood Johnson Medical School, New Brunswick, New Jersey; and [4]Department of Hematology, Huashan Hospital, Shanghai Medical College, Fudan University, Shanghai, P.R. China

Received 4/1/08; revised 9/23/08; accepted 9/24/08; published OnlineFirst 01/27/2009.

Grant support: National Foundation for Cancer Research.

The costs of publication of this article were defrayed in part by the payment of page charges. This article must therefore be hereby marked *advertisement* in accordance with 18 U.S.C. Section 1734 solely to indicate this fact.

Note: Supplementary data for this article are available at Clinical Cancer Research Online (http://clincancerres.aacrjournals.org/).

Requests for reprints: Tulin Budak-Alpdogan, The Cancer Institute of New Jersey, 195 Little Albany Street R4511, New Brunswick, NJ 08903. Phone: 732-235-9836; Fax: 732-235-8681; E-mail: budaktu@umdnj.edu.

©2009 American Association for Cancer Research.

doi:10.1158/1078-0432.CCR-08-0810

Downloaded from clincancerres.aacrjournals.org on September 26, 2020. © 2009 American Association for Cancer Research.

Translational Relevance

In extensive-stage small-cell lung cancer (SCLC), chemotherapy response provides only a modest change in survival. The retinoblastoma (pRb) tumor suppressor gene, the master regulator of the G_1-S phase transition, is inactivated in more than 90% of SCLC. Flavopiridol has limited value as a single agent in cancer treatment but it is effective when combined with other chemotherapeutic agents. Doxorubicin is a widely used chemotherapeutic for SCLC. In this article, we show that flavopiridol pretreatment makes pRb-negative SCLC cells more sensitive to doxorubicin both *in vitro* and *in vivo* while decreasing toxicities to normal renewal tissues.

To the patients who failed to respond to first- and/or second-line treatments for SCLC, doxorubicin-containing regimens exert substantial toxicity risk. Decreasing the extent of toxicity while increasing antitumor response with low-dose flavopiridol and doxorubicin combination might provide some survival benefit to these heavily pretreated patients.

enzyme topoisomerase II that unwinds DNA for transcription. Doxorubicin-stabilized topoisomerase II complex prevents resealing of the DNA double helix. Irreparable DNA damage induces p53 activation and consequently apoptosis (14). Doxorubicin cytotoxicity mechanisms also involve inhibition of RNA polymerase and cytochrome *c* oxidase, and chelation of iron and generation of reactive oxygen species (15).

Flavopiridol is a novel flavone that inhibits multiple cyclin-dependent kinases (CDK) that govern cell cycle progression at the G_1-S and G_2-M boundaries (16–19). Flavopiridol is an antiproliferative and an apoptotic agent that also has anti-angiogenic properties (5, 20–23).

We previously reported in a sarcoma model that flavopiridol blocked pRb-expressing cells (i.e., normal replicating cells) at the G_1-S boundary, whereas the cells lacking pRb or with nonfunctional pRb kept cycling (24). Therefore, cells with pRb were protected from the effects of doxorubicin after flavopiridol pretreatment, whereas cells lacking pRb were not. The flavopiridol then doxorubicin treatment combination had a synergistic cytotoxic effect on pRB lacking human osteosarcoma cell line (SaOs-2) whereas their pRb-expressing counterparts had a G_1 arrest with flavopiridol exposure and had a decreased cytotoxic response to following doxorubicin exposure (24).

The purpose of the present study was to test this observation in SCLC, with particular reference to induction of synergistic cell kill in a *de novo* pRb-negative cell line, H69, and a pRb-expressing cell line, H865, and a pRb small interfering RNA (siRNA) knockdown H865 clone. We show that *de novo* SCLC cells are relatively sensitive to both flavopiridol and doxorubicin, and flavopiridol and doxorubicin combinations exert both *in vitro* and *in vivo* synergistic effects. Ablating the Rb expression in H865 cell line with stable pRb siRNA transfection did not alter tumor growth kinetics neither *in vitro* nor *in vivo* and the relative drug sensitivity of the cell lines; however, the H865 pRb knockdown cell line gained significant sensitivity to the sequential flavopiridol-doxorubicin combination.

Materials and Methods

Cell lines and drugs. A SCLC cell line, NCI H69, that lacked pRb was purchased from the American Type Culture Collection and was cultured in RPMI 1640 (Life Technologies) supplemented with 2 mmol/L L-glutamine, 1.5 g/L sodium bicarbonate, 4.5 g/L glucose, 10 mmol/L HEPES, 1.0 mmol/L sodium pyruvate, and 10% heat inactivated fetal bovine serum (FBS). The NCI H865 cell line, expressing functional pRb, was generously provided by Adi Gazdar (Southwestern Medical Center at Dallas, Dallas, TX) and was cultured in DMEM/F-12 containing 10% FBS.

Flavopiridol was obtained from the Cancer Therapy Evaluation Program as a pure powder, and doxorubicin hydrochloride was obtained from Sigma-Aldrich Co. Both drugs were dissolved in DMSO and stock solutions were stored at -20°C.

Retinoblastoma gene knockdown in the H865 cell line. The H865 cell line was transduced with Rb-specific siRNA coding pFIV U6/H1 vector (System Biosciences) to generate stable pRb-negative H865 clones. Two different siRNA sequences known to down-regulate Rb mRNA >90% were chemically synthesized (25). The sequences for the siRNA template were as follows: (*a*) 5′-aaagGATACCAGATCATGTCAGA-3′, 3′-CTATGGTCTAGTACAGTCTaaaa-5′ and (*b*) 5′-aaagCCCAGCAGTTC-GATATCTA-3′, 3′-GGGTCGTCAAGCTATAGATaaaa-5′. Oligonucleotides were annealed, phosphorylated, and then inserted into pFIV-H1/U6 siRNA expression vector that contained both ampicillin and puromycin resistance genes (System Biosciences). Vector siRNA template insertions were confirmed with sequencing. 293TN cells were transfected with pPACK packaging plasmid mix and lentiviral siRNA constructs using Lipofectamine (Invitrogen Corporation). The pFIV U6/H1 construct expressing siRNA against luciferase mRNA was used as a control. All vectors were pseudotyped with vesicular stomatitis virus G protein envelope.

The H865 cell line was transduced with high-titer vector stocks (>10^7 tu/mL) in the presence of polybrene (8 μg/mL), and then single cell–derived clones were generated with puromycin (4 μg/mL) selection. Seventeen clones were picked with cloning rings and their genomic DNA was isolated. Vector insertion was evident in all of the clones with woodchuck hepatitis virus posttranscriptional regulation element (WPRE)–specific PCR. The primers for PCR were as follows: forward primer 5′-TCATGCTATTGCTTCCCGTATGGCTTTC-3′, and reverse primer 5′-GGATTGAGGGCCGAAGGGACGTAG-3′.

In vitro ***cytotoxicity assay.*** For single-drug cytotoxicity, cells were plated in 96-well plates as follows: 1×10^4 per well for H865 parental cell line and its derivatives and 5×10^4 per well for H69. Serial dilutions of each drug or equivalent volumes of DMSO were then added in quadruplicate to the plates. After 24 h of treatment, drugs were removed and cells were incubated in a drug-free medium for 3 more days. On day 5, tetrazolium compound [3-(4,5-dimethylthiazol-2-yl)-5-(3-carboxymethoxyphenyl)-2-(4-sulfophenyl)-2*H* tetrazolium, inner salt; MTS] and the electron coupling reagent phenazine methosulfate were added to the wells according to the manufacturer's protocol (Promega Co.). After 4 to 6 h of incubation, a microplate reader (Molecular Devices Corp.) was used to read the absorbance of the wells at 492 nm. Inhibitory concentration values at 50% (IC_{50}) were calculated with Hill's equation by using the Graph Pad Prism software v3.0.

The effect of sequential exposure to flavopiridol and doxorubicin was assessed by exposing cells to graded concentrations of drugs at fixed ratios. The schedules tested were as follows: (*a*) flavopiridol for 24 h and then doxorubicin for 24 h; (*b*) doxorubicin for 24 h and flavopiridol for 24 h; and (*c*) flavopiridol for 24 h, 2 d of washout period and then doxorubicin for 24 h. Fixed ratios were flavopiridol IC_{10} and doxorubicin IC_{50}, or flavopiridol IC_{25} and doxorubicin IC_{50}. Serial dilutions of drug concentrations were done as follows: flavopiridol (1/8, 1/4, 1/2, 1, 2, 4, 8 $\times IC_{10}$) and doxorubicin (1/8, 1/4, 1/2, 1, 2, 4, 8 $\times IC_{50}$). The fractional survival for each combination was calculated by dividing the mean absorbance value

Downloaded from clincancerres.aacrjournals.org on September 26, 2020. © 2009 American Association for Cancer Research.

of drug-treated wells to the mean absorbance value of control wells. The median effect lines were analyzed by the method of Chou and Talalay, using CalcuSyn software (Biosoft; ref. 26). Combination index (CI) values were calculated under the assumption that drugs act at different targets (i.e., mutually nonconclusive drug interaction). With this methodology, synergy was indicated by CI < 1, additive by CI = 1, and antagonism by CI > 1. For combination experiments, each condition had six to eight replicate wells and experiments were repeated at least thrice (correlation coefficients for median-effect lines >0.9).

Western blot analysis. The clones were then tested for pRb expression with Western blotting. Cell lysate proteins were separated by 8% SDS-PAGE and then transferred to Westran S polyvinylidene difluoride membranes (Whatman). After blocking with 5% nonfat dried milk solution, the membranes were incubated first with primary antibodies (i.e., mouse monoclonal IgG1 to pRb, Santa Cruz Biotechnology) or purified mouse anti-human underphosphorylated pRb or polyclonal α-tubulin antibody (Sigma Chemical Co.), and then with secondary antibody, goat anti-mouse IgG (Santa Cruz Biotechnology), conjugated to horseradish peroxidase. The blots were visualized by enhanced chemiluminescence detection kit (Amersham Biosciences). We compared the Rb protein levels from different clones by using chemiluminescence detection (ChemiDoc XRS; Bio-Rad Laboratories) and Quantity One 1-D Analysis software.

Cell cycle analysis. H69, H865 parental, and H865 Rb siRNA clone 12 cells were dispersed into 12-well plates (2×10^5/well, triplicate) 24 h before exposure to flavopiridol and doxorubicin. Single drug exposures were for 24 h and then cells were transferred into fresh growth medium. For combination studies, flavopiridol and doxorubicin doses were scheduled as IC_{25} of flavopiridol day 1 and IC_{50} doxorubicin on day 2 (flavopiridol then doxorubicin) or in reverse order (doxorubicin then flavopiridol). Following drug treatment, cells were harvested at either 48 or 72 h time points and then stained with propidium iodide/RNase staining buffer (BD Pharmingen) according to the manufacturer's protocol. Samples were acquired with a FACSort flow cytometer (Becton Dickinson) and then the DNA distribution for cell cycle analysis was determined with ModFit v3.0 software (Becton Dickinson).

Annexin V staining for apoptosis. Apoptotic populations of the H865 parental and pRb knockdown clone 12 cell lines were compared after drug exposure in three independent experiments. Flavopiridol and doxorubicin single drug incubations were limited to 24 h, and for combinations each drug exposure was also 24 h. At the end of 48 h, all samples were harvested and washed with PBS. For each condition, 10^5 cells were stained with 5 μL Annexin V-FITC (BD Pharmingen) and 5 μL 7-amino-actinomycin D (BD Pharmingen, Franklin Lanes NJ). Cells were then analyzed with a FACSort flow cytometer (Becton Dickinson). The percentage of early apoptotic cells was determined as percentage of Annexin V-FITC–positive but 7-amino-actinomycin D–negative cell populations using the CellQuest software.

In vivo *studies.* Athymic nude male mice were purchased from The Jackson Laboratory at 5 to 6 wk age. When the animals were 7 to 8 wk old, they were injected with human NCI-H69 (pRb negative), parental H865 (pRb positive), or pRb siRNA–transduced H865 cells (clone 12). A suspension of 10^7 cells in 0.1 mL of RPMI 1640 was injected s.c. into the right flanks of mice. In 2 wk when the tumor diameters reached ~0.5 cm, the mice were randomly assigned into six groups: (*a*) group 1, control (no drugs, 1.0% DMSO/sodium chloride solution); (*b*) group 2, flavopiridol (5 mg/kg/d, every other day for 3 d); (*c*) group 3, doxorubicin (4 mg/kg/d, every other day for 3 d); (*d*) group 4, flavopiridol (5 mg/kg/d, on days 1, 3, and 5) followed by doxorubicin

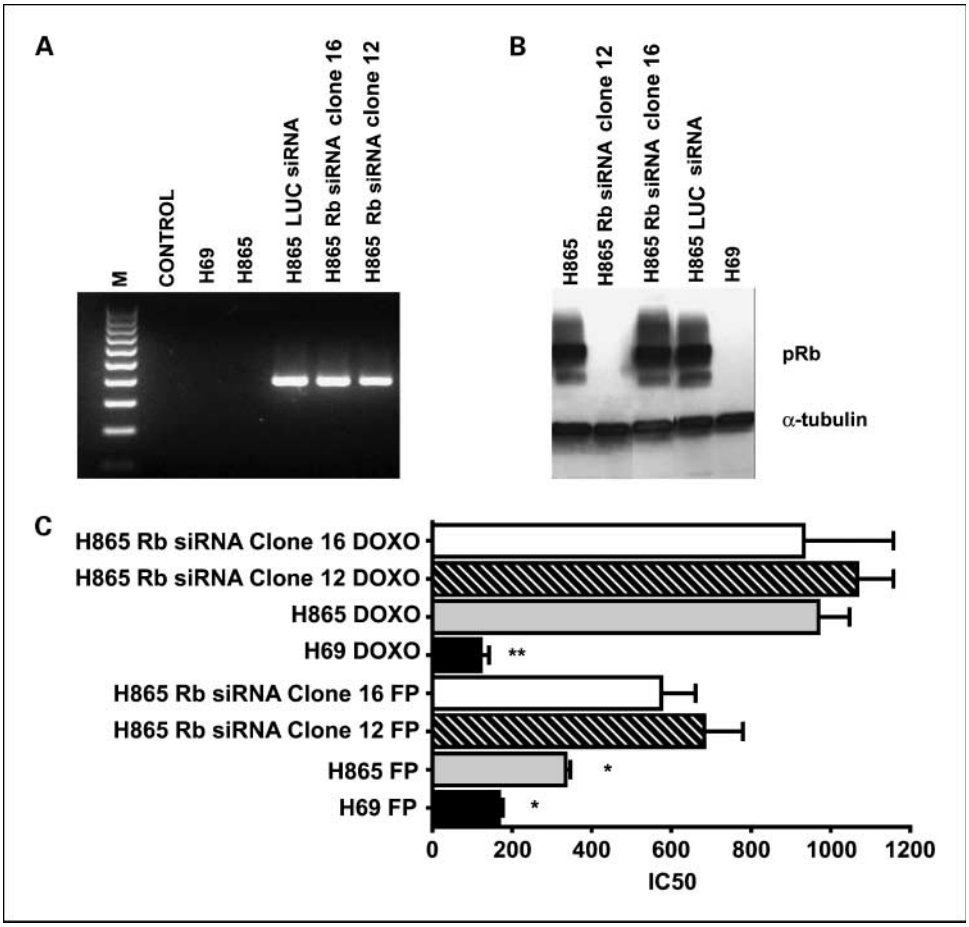

Fig. 1. Molecular and drug sensitivity characteristics of SCLC cell lines; H69-, H865-, and H865-derived cell lines carrying either luciferase (*LUC*) control siRNA or retinoblastoma (*Rb*) siRNA. *A,* PCR for WPRE; no template control, H69, and parental H865 samples were negative for any amplification band, and all puromycin-selected H865-derived clones had the expected 400-bp WPRE band. *B,* Western blots with primary antibody against hypophosphorylated Rb protein; H865 parental cell line, H865 Luc control siRNA clone, and H865 Rb siRNA clone 16 were positive for retinoblastoma protein, whereas the H69 cell line and H865 Rb siRNA clone 12 lacked the Rb protein band. α-Tubulin immunoblotting was used as loading control. *C,* mean IC_{50} values from three independent experiments for flavopiridol (*FP*) and doxorubicin (*DOXO*): solid black, H69; solid gray, H865; striped, H865 Rb siRNA clone 12 with no Rb protein; solid white, H865 Rb siRNA clone 16 with Rb protein. H69 was the most sensitive cell line among H865 and its derivatives for both flavopiridol and doxorubicin. Lentiviral gene transfer did not alter doxorubicin sensitivity of the H865 cell line. Drug exposure for both drugs was 24 h.

Downloaded from clincancerres.aacrjournals.org on September 26, 2020. © 2009 American Association for Cancer Research.

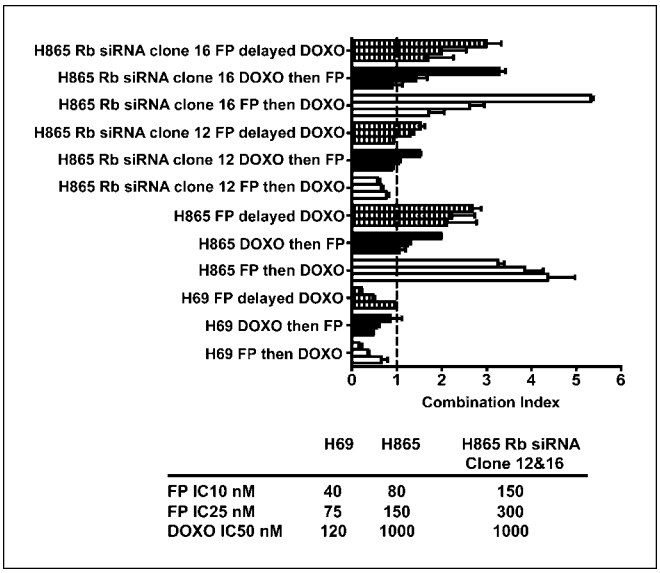

	H69	H865	H865 Rb siRNA Clone 12&16
FP IC10 nM	40	80	150
FP IC25 nM	75	150	300
DOXO IC50 nM	120	1000	1000

Fig. 2. The effect of sequential exposure on the cytotoxic interaction between flavopiridol and doxorubicin was tested on Rb-positive (H865 and H865 Rb siRNA clone 16) and Rb-negative (H69 and H865 Rb siRNA clone 12) SCLC cell lines. Drug doses that are used for combination studies are summarized as text under the graph. Combination index values for different sequences are indicated as follows: FP then DOXO, 24 h flavopiridol followed by 24 h doxorubicin; DOXO then FP, 24 h doxorubicin followed by 24 h flavopiridol; FP delayed DOXO, 24 h flavopiridol, 48 h washout then 24 h doxorubicin. Columns, means of at least three independent experiments; bars, sample SE. For each group, the combination indexes for different values of fractions affected (Fa) are represented in the following order: bottom row, 50% Fa; middle row, 75% Fa; top row, 95% Fa.

(4 mg/kg/d, on days 2, 4 and 6); (*e*) group 5, doxorubicin (4 mg/kg/d, on days 1, 3, and 5) followed by flavopiridol (5 mg/kg/d, on days 2, 4, and 6); and (*f*) group 6, flavopiridol (5 mg/kg/d, on days 1, 5, and 9) followed by delayed doxorubicin (4 mg/kg/d, on days 4, 8, and 12) exposure. Tumor size and body weight were assessed every other day. Tumor volume was calculated as tumor volume (mm^3) = length × $(width)^2/2$. Toxicity was monitored by weight loss. Mice were sacrificed when the diameter of tumor exceeded 1.5 cm.

We used the Cox proportional hazards models to model the survival of the animals (27). All models were fitted using the R statistical system version 2.6.0 (28). For comparing the effects of drug treatment modalities on tumor growth, we calculated the time to reach 1.5 cm^3 tumor volume for each animal, and the mean values for each group were compared by one-way ANOVA test and Bonferroni's multiple comparison test. However, substantial toxicity of certain drug treatment options and toxicity-related animal deaths required analyzing the data further for understanding the survival differences among groups. We considered two outcome measures that were measured over time in each animal: tumor volume and total body weight change as a percentage of the initial animal weight. The tumor volume measurements were log transformed to enable the fitting of linear relationships of this variable with time. To account for repeated measurements on individual animals and for the variability of the outcome/time relationships from animal to animal, we used random-effects models (29). Slopes and 95% confidence intervals for linear relationships of each of the two variables and for each of the six treatments with respect to time were computed from the fitted models.

Results

Expression of pRb in SCLC cell lines. All three PCR reactions with WPRE, U6/H1, and puromycin resistance gene–specific primers (data are not shown for the last two primer sets) were positive for all vector-transduced H865 clones and negative for H69 and parental H865 cell lines. Figure 1A depicts the PCR reaction for WPRE, including control, H865 luciferase (Luc) siRNA clone, and H865 Rb siRNA carrying clones 16 and 12.

Out of 17 H865 Rb siRNA clones, only two (clones 12 and 17) had undetectable levels of Rb protein, whereas the other 15 clones had pRb levels of 5% to 100% compared with the pRb level of the original H865 cell line. Western blot analysis revealed that parental H865, the control Luc siRNA-transduced H865 clone, and the Rb siRNA-transduced clone 16 expressed pRb whereas H69 cells and H865 Rb siRNA clone 12 had undetectable levels of Rb protein (Fig. 1B).

Flavopiridol and doxorubicin sensitivity of the cell lines. Flavopiridol has been reported to induce growth inhibition and cytotoxicity in SCLC cell lines (30). The loss of cell cycle regulation in SCLC cells, largely due to loss of Rb function, results in a defective G_1-S restriction point in these cells and makes them unresponsive to normal cell cycle regulation. Inhibiting the CDK pathway with flavopiridol interferes with cell cycle progression in these cells and induces either a cytostatic or an apoptotic effect. SCLC cell lines have been observed to be highly sensitive to flavopiridol-induced apoptosis. In our study, the *de novo* Rb-negative cell line H69 was the most sensitive cell line to both flavopiridol (IC_{50} 167.5 ± 24.5 nmol/L) and doxorubicin (IC_{50} 121.4 ± 41.1 nmol/L; Fig. 1C).

The IC_{50} values for doxorubicin for the parental H865 cell line and its derivative clones with FIV integration were similar (970 ± 133.3, 1,067 ± 90.3, and 932 ± 225.7 nmol/L for H865 parental, H865 Rb siRNA clone 12, and H865 Rb siRNA clone 16, respectively). However, FIV-integrated H865 clones became more resistant to flavopiridol than the parental H865 cell line (Fig. 1C; $P < 0.03$). The H865 cell line transduced with control Luc siRNA FIV was also more resistant to flavopiridol (IC_{50} 750 ± 187 nmol/L) than the parental H865 cell line, whereas doxorubicin sensitivity was not significantly different from the other H865 cell lines (IC_{50} 1,297 ± 345 nmol/L, $P = 0.626$).

Sequential flavopiridol and doxorubicin combination has a synergistic cytotoxic effect on Rb-negative SCLC cell lines. Flavopiridol combinations with a variety of chemotherapeutic agents are observed to have either synergistic or antagonistic effects depending on their administration schedule (31). Flavopiridol administration preceding doxorubicin was observed to result in synergistic cell kill in an osteosarcoma cell line (24). The effect of sequential administration on the cytotoxic interaction between flavopiridol and doxorubicin was tested with three different schedules: 24 hours of flavopiridol and then 24 hours of doxorubicin exposure, doxorubicin then flavopiridol exposure in reverse order, and 24 hours of flavopiridol followed by 48-hour washout period and then 24 hours of doxorubicin exposure. For combination studies, fixed drug IC_x ratios were as follows: flavopiridol IC_{10} and doxorubicin IC_{50}, or flavopiridol IC_{25} and doxorubicin IC_{50}. Figure 2 presents the results for flavopiridol IC_{25} and doxorubicin IC_{50} fixed ratios but the other drug combination ratio (flavopiridol IC_{10} and doxorubicin IC_{50}) had similar results (data not shown). Combination indexes presented in Fig. 2 are the means of three independent experiments and each experimental plate had six to eight replicates for each serial dilution point. In the H69 cell line, all flavopiridol and

Downloaded from clincancerres.aacrjournals.org on September 26, 2020. © 2009 American Association for Cancer Research.

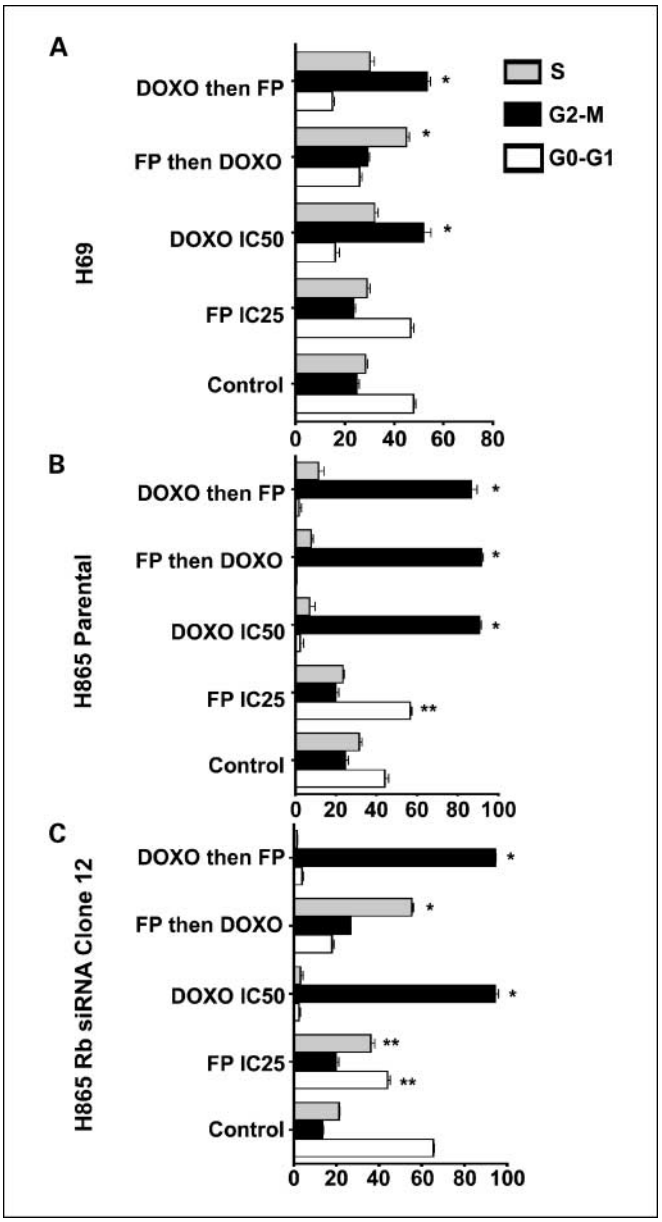

Fig. 3. Cells were exposed to either relevant flavopiridol IC_{25} or doxorubicin IC_{50} doses alone for 24 h or their sequential combinations: flavopiridol then doxorubicin or doxorubicin then flavopiridol. *A,* cell cycle distribution results of three independent experiments; bars, SE for the H69 cell line. Doxorubicin alone and doxorubicin then flavopiridol treatment options showed statistically significant ($P < 0.03$) G_2-M accumulation, whereas only flavopiridol then doxorubicin treatment accumulated the cells in the S phase. The columns that are statistically different are marked with an asterisk. *B,* the cell cycle distribution results of three independent experiments; bars, SE for H865 parental cell line. All doxorubicin-containing treatment modalities instigated statistically significant ($P < 0.02$) G_2-M accumulation (*), whereas flavopiridol alone triggered G_0-G_1 accumulation (**). *C,* cell cycle distribution results of three independent experiments; bars, SE for H865 Rb siRNA clone 12 with no Rb protein. Doxorubicin alone and doxorubicin then flavopiridol treatment options showed statistically significant ($P < 0.03$) G_2-M accumulation, whereas flavopiridol then doxorubicin treatment accumulated the cells in the S phase. These columns are marked with an asterisk. Additionally, flavopiridol-alone treatment resulted in a statistically significant G_0-G_1 decrease and S phase ($P < 0.05$) increase (**).

doxorubicin combinations were synergistic; however, in the H865 Rb siRNA clone 12, the greatest reduction in IC_{50} values were observed when 24 h of flavopiridol incubation was followed by 24 h of doxorubicin exposure. Meanwhile, for all Rb protein–expressing cells [i.e., H865 parental, H865 with Luc siRNA (data not shown), and H865 Rb siRNA clone 16], all flavopiridol and doxorubicin combinations were antagonistic (Fig. 2). Although the flavopiridol sensitivity of the H865-derived cell lines was decreased, the Rb knockdown H865 derivatives became more sensitive to the flavopiridol and doxorubicin combination.

The flavopiridol and doxorubicin combination induces different cell cycle changes in Rb-negative and Rb-positive SCLC cell lines. To explore the cell cycle effects of flavopiridol and doxorubicin and their combination, H69 (Supplementary Fig. S1A-E), H865 Rb siRNA clone 12 (Supplementary Fig. S1F-J), and H865 parental cells (Supplementary Fig. S1K-O) were treated with flavopiridol IC_{25} alone, doxorubicin IC_{50} alone, flavopiridol IC_{25} then doxorubicin IC_{50}, or doxorubicin IC_{50} then flavopiridol IC_{25}. Cell line relevant IC_{25} and IC_{50} values that were used in these experiments were similar to flavopiridol and doxorubicin doses summarized in Fig. 2. Cells were stained with propidium iodide at the 6-, 12-, 24-, 48-, and 72-hour time points; the 48-hour time point results are shown in Fig. 3. In all cell lines, doxorubicin alone induced a substantial increase in the percent of cells in G_2-M (Fig. 3A-C; $P < 0.01$). In the H865 parental cell line, flavopiridol induced G_1 accumulation (G_1 fraction for control and flavopiridol treated cells were 44 ± 2% and 56.6 ± 0.8%, respectively) starting from as early as 24 hours ($P < 0.05$). None of the flavopiridol and doxorubicin combination sequences were able to change doxorubicin-triggered G_2-M accumulation in the H865 parental cell line. In contrast, flavopiridol did not alter the cell cycle distribution of the Rb-negative H69 cells. Cell

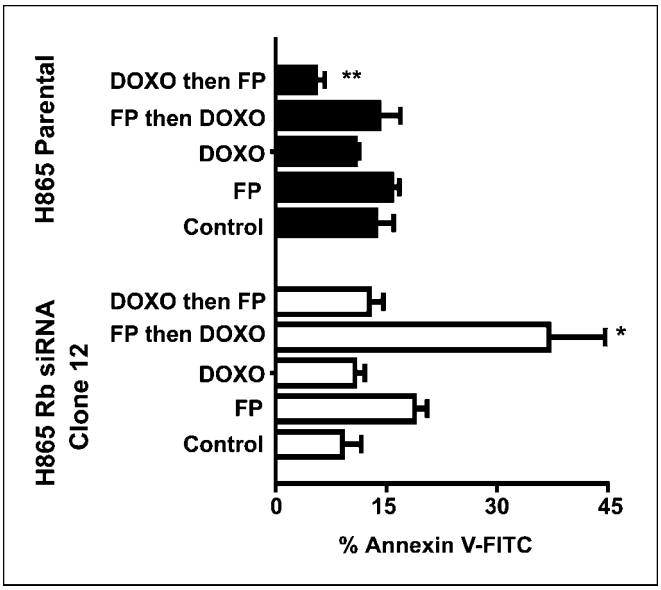

Fig. 4. Apoptosis was quantitated at 48 h by staining SCLC cell lines with 7-amino-actinomycin D and Annexin V-FITC. Cells were exposed to either flavopiridol or doxorubicin for 24 h, and for sequential combination studies 24 h of one drug exposure and washout was followed by 24 h of exposure to the second drug. This graph summarizes the results of three independent experiments; bars, SE. H865-Rb knockdown cell line (*solid white columns*) had the highest apoptosis induction with treatments compared with H865 parental cells (*solid black columns*). The most significant difference was observed when flavopiridol treatment preceded doxorubicin exposure ($P < 0.02$; *). In H865 parental cells, doxorubicin then flavopiridol treatment decreased apoptosis ($P < 0.05$; **).

Downloaded from clincancerres.aacrjournals.org on September 26, 2020. © 2009 American Association for Cancer Research.

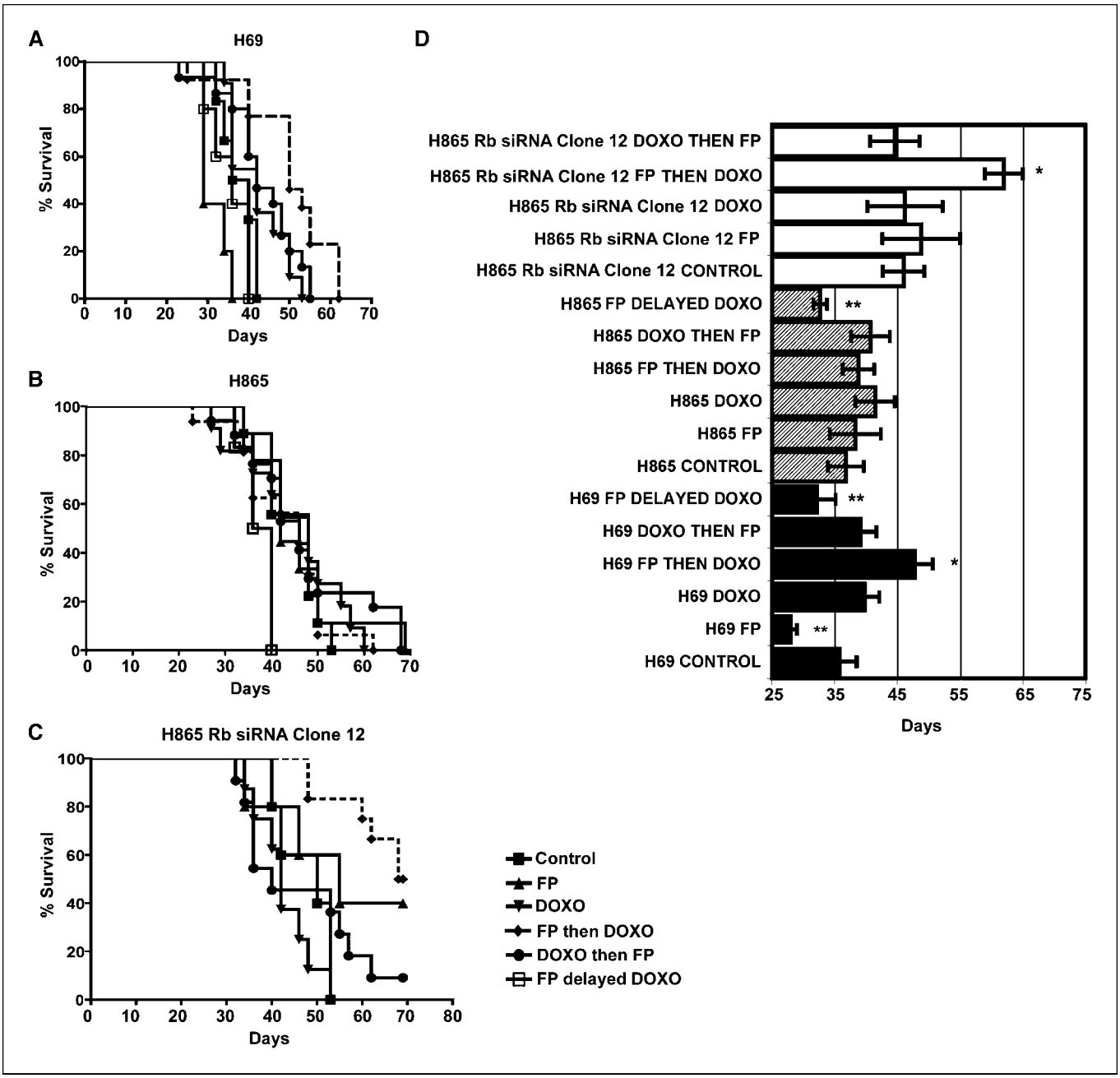

Fig. 5. Survival curves and treatment responses of nude mice bearing human SCLC tumors. *A,* H69 tumor-bearing animals were followed after no treatment (■, $n = 6$, median survival 38 d), flavopiridol alone (▲, $n = 5$, median survival 29 d), doxorubicin alone (▼, $n = 11$, median survival 42 d), flavopiridol then doxorubicin (♦, $n = 13$, median survival 50 d), doxorubicin then flavopiridol (●, $n = 15$, median survival 42 d), or flavopiridol then delayed doxorubicin (□, $n = 5$, median survival 36 d). The flavopiridol then doxorubicin treatment sequence provides a better survival for animals bearing the H69 tumor (with Cox proportional hazards model $P = 0.00051$). *B,* H865 tumor-bearing animals were followed after no treatment (■, $n = 9$, median survival 48 d), flavopiridol alone (▲, $n = 9$, median survival 42 d), doxorubicin alone (▼, $n = 11$, median survival 48 d), flavopiridol then doxorubicin (♦, $n = 16$, median survival 46 d), doxorubicin then flavopiridol (●, $n = 17$, median survival 46 d), or flavopiridol then delayed doxorubicin (□, $n = 6$, median survival 38 d). *C,* H865-Rb siRNA knockdown tumor-bearing animals were followed after no treatment (■, $n = 5$, median survival 50 d), flavopiridol alone (▲, $n = 8$, median survival 42 d), doxorubicin alone (▼, $n = 11$, median survival 48 d), flavopiridol then doxorubicin (♦, $n = 12$, median survival 68.5 d), or doxorubicin then flavopiridol (●, $n = 11$, median survival 40 d). The flavopiridol then doxorubicin treatment sequence provides a better survival in this model (with Cox proportional hazards model $P = 0.0023$). *D,* treatment modalities are compared by calculating the median time to reach a tumor volume of 1.5 cm^3. Delayed flavopiridol then doxorubicin treatment modality had an adverse effect on tumor growth control both in the H69 and H865 xenograft models ($P < 0.05$). Flavopiridol followed by doxorubicin provided better tumor growth control for only Rb-negative SCLC models, H69, and H865 Rb0 ($P < 0.05$).

cycle modeling of the ModFit program failed to detect the flavopiridol then doxorubicin combination–induced G_1-S block in Rb-negative cell lines. The combination triggered both apoptotic sub-G_1 and shifted S-phase peaks that substantially overlapped with the G_1 peak (Supplementary Fig. S1D). There was a prominent shift of the channels corresponding to N and 2N compared with the other H69 cell cycle plots. Nevertheless, flavopiridol then doxorubicin induced prominent S-phase accumulation in H69 cells (Fig. 3A). In the H865 Rb siRNA clone 12 Rb, doxorubicin alone and doxorubicin followed by

Downloaded from clincancerres.aacrjournals.org on September 26, 2020. © 2009 American Association for Cancer Research.

flavopiridol exposure resulted in a G_2-M block (Fig. 3C); however, interestingly, these cells responded to flavopiridol then doxorubicin treatment with a G_1-S accumulation, similar to H69 cells.

Flavopiridol then doxorubucin exposure induces the highest amount of apoptosis in the Rb knockdown H865 cell line. Flavopiridol then doxorubicin treatment–related cell cycle changes, in conjunction with summarized *in vitro* synergism data, made us inquire as to whether this flavopiridol dysregulated G_1-S transition was increasing the doxorubicin exposure of the cells and subsequently increasing DNA damage–induced apoptosis.

Apoptotic populations of the H865 parental and its Rb knockdown derivative cell line were compared after flavopiridol and/or doxorubicin exposure (Fig. 4). H865 Rb siRNA clone 12 and H865 parental cells were treated with flavopiridol IC_{25} alone, doxorubicin IC_{50} alone, flavopiridol IC_{25} then doxorubicin IC_{50}, or doxorubicin IC_{50} then flavopiridol IC_{25}. The cells were exposed to the same drug doses that were summarized in Fig. 2. Flavopiridol exposure induced statically significant apoptosis in only the H865 Rb siRNA clone 12 (upon flavopiridol exposure the apoptotic cell population increased from 9.1 $\pm$ 2.5% to 18.8 $\pm$ 1.7%), but the most marked change was with flavopiridol then doxorubicin sequential treatment (apoptotic population increased to 37 $\pm$ 7.7%; $P < 0.02$; Fig. 4). Treatment did not alter the apoptotic cell populations for H865 parental cells; however, interestingly, we observed less apoptosis (5.4 $\pm$ 1.2%) with the doxorubicin then flavopiridol sequence in the parental cell line (Fig. 4).

We performed similar apoptosis experiments with the H69 cell line; however, they were very sensitive to the Ca^{2+}-containing Annexin V binding buffer, and even nontreated cells lost 75% of their viability within 15 minutes of incubation time.

Therapeutic efficiency of sequential flavopiridol and doxorubicin in nude mice bearing human SCLC xenografts. *In vivo* growth kinetics of the cell lines H69, H865 parental, and H865 Rb siRNA clone 12 were different from their *in vitro* growth patterns. H69 cells grow dominantly as spheres in culture and their generation time varies between 4 and 5 days. This cell line is well known for its extracellular matrix dependence for survival (32). H69 cells grew faster *in vivo* than the other two cell lines after injection of 10^7 cells, although both of the H865 cell lines have an average generation time of 2 days *in vitro*. The animals bearing the H69 tumor had a median survival of 38 days, whereas the animals with either H865 parental or H865 Rb siRNA clone 12 had median survivals of 42 and 50 days, respectively. In both H69 and H865 Rb siRNA clone 12 xenograft models, flavopiridol then doxorubicin treatment modality provided the longest median survivals of 50 and 68.5 days, respectively (Fig. 5A and C; $P < 0.001$ and $P < 0.003$, respectively). We calculated the change in tumor size in log volume per day with a random-effects model, as well as mean time to reach 1.5 cm^3 tumor volume (Fig. 5D). For the H69 xenograft, treatment with flavopiridol alone treatment modality had the steepest log tumor volume change per day (mean 0.22 per day with a 95% confidence interval range of 0.186-0.257 per day), whereas flavopiridol followed by delayed doxorubicin had similar log volume change as the control (0.20 and 0.197 per day, respectively). Doxorubicin alone treatment decreased the growth rate to 0.17 log tumor volume change per day (95% confidence interval range of 0.145-0.19 per day). Flavopiridol/doxorubicin combinations had similar log volume changes of 0.15 ($P < 0.05$) that were significantly lower than the other groups. However, doxorubicin then flavopiridol treatment (-0.30 log percent weight change per day, range -0.4 to -0.20 per d) was more toxic ($P < 0.01$) than both doxorubicin alone (-0.175 per day with a range of -0.29 to -0.06 per day) and flavopiridol then doxorubicin sequential combination (-0.24 per day with a range of -0.34 to -0.19 per day).

For *in vivo* studies, a nontoxic flavopiridol dose that would induce mainly a G_1 block was used. We did not observe any overt total body weight loss with flavopiridol treatment in any of the xenograft models. Flavopiridol treatment alone did not alter the tumor growth rate in the H865 xenografts and slightly increased the tumor growth rate in the H69 model ($P < 0.03$; Fig. 5A-D). Doxorubicin alone (-0.42 per day, with a range of -0.60 to -0.25 per day percent weight change in log) and doxorubicin then flavopiridol treatment (-0.55 per day, with a range of -0.70 to -0.39 per day) modalities were the most toxic treatment modalities in the H865 Rb0 model ($P < 0.001$). Flavopiridol then doxorubicin treatment had less toxicity than doxorubicin then flavopiridol treatment in both H69 and H865 Rb knockdown models. Although the flavopiridol then delayed doxorubicin sequencing had less toxicity than the other sequential treatments, this sequence did not show significant tumor growth control in any of the tumor models (Fig. 5D). In the H865 parental xenograft model, tumor growth and survival rates of the drug treatment groups were similar to that of the no treatment group ($P > 0.05$; Fig. 5B and D).

Therefore, we observed a significant survival advantage in Rb-negative SCLC xenograft models with the sequential flavopiridol then doxorubicin treatment program, as a result of its better tumor growth delay as well as less toxicity.

Discussion

SCLC cells are not only devoid of G_1-S cell cycle restriction point due to loss of functional retinoblastoma protein expression, but may also have a defective G_1-S DNA damage check point, and defective G_2-M and M check points, due to loss of p53 function, mutation, or aberrant methylation of the different checkpoint regulator genes (7, 8). This high degree of variability of cell cycle components and their regulators in SCLC makes the predictions about response to cell cycle–directed agents very complex. Almost 60% to 80% of the SCLC patients express abnormal p53 without any chemotherapy response correlation or prognostic significance (33) and *in vitro*, wild-type p53 restoration does not modify the sensitivity of a lung cancer cell line to a given chemotherapeutic agent (34). Flavopiridol is known to induce apoptosis in certain cell types independent of Rb and p53 pathway alterations (35, 36). As a single agent, flavopiridol has unsatisfactory or limited value in cancer treatment but it has been observed to be most effective when combined with other chemotherapeutic agents (21, 37–41). Flavopiridol not only disrupts cell cycle progression by interfering with the CDK cascade but also reduces the levels of different antiapoptotic proteins (42–47). SCLC cell lines have been noticed to have enhanced sensitivity to flavopiridol exposure relative to non-SCLC cell lines (30, 36).

Downloaded from clincancerres.aacrjournals.org on September 26, 2020. © 2009 American Association for Cancer Research.

Flavopiridol could also induce apoptosis in primary cells, but that dose is usually much higher than the dose required for SCLC apoptosis (30). SCLC cells have defects in both G_1-S and G_2-M checkpoint regulation, and S-phase synchronization increases flavopiridol-induced apoptosis in SCLC cell lines (30). In the presence of functional pRb, inhibition of the CDK cascade, i.e., cyclin D1/cdk4,6 or cyclinE/cdk2, by CDK inhibitors dominantly arrest the cells at G_1 and makes them less responsive to S-phase–acting agents (31). In cells that display a high-grade G_1 arrest with flavopiridol, like our H865 parental model, the response to drug treatment was observed to be more cytostatic rather than apoptotic (30). Doxorubicin is known to have significant activity in SCLC, alone or in combination (48–50). With this knowledge, we aimed to combine flavopiridol and doxorubicin so that the effects of either agent are not inhibited but rather augmented.

We previously observed in pRb-negative osteosarcoma cells (SaOs-2) that flavopiridol pretreatment made them more sensitive to doxorubicin, whereas a subline that was transfected with pRb arrested at G_1-S with flavopiridol treatment and had decreased cytotoxicity to doxorubicin (24). These observations encouraged us to test the efficiency of different flavopiridol and doxorubicin combinations in SCLC, a tumor that has a high frequency of pRB loss. The proposed mechanism was that in the presence of an intact G_1-S checkpoint, cells with functional pRb would be blocked in G_1-S by flavopiridol and subsequent exposure to doxorubicin would have a lessened effect as the drug exerts its maximum toxicity in late S-G_2. Furthermore, as normal renewal tissue cells also have an intact G_1-S checkpoint, toxicity to these tissues might also be lessened.

Cell cycle data showed substantial S-phase accumulation and apoptotic sub-G_1 population with this schedule, but because of innate sensitivity of the H69 cell line to the Annexin binding buffer, we were not able to quantitate apoptosis with Annexin V staining. It is known that *in vitro* survival of H69 cells increases in the presence of extracellular matrix proteins, and they become less sensitive to chemotherapeutics (32). In the nude mouse-human H69 xenograft model, flavopiridol alone treatment and the schedule of flavopiridol then delayed doxorubicin were the worst in terms of tumor volume control, but were also the least toxic. The doxorubicin then flavopiridol schedule exerted some *in vitro* synergism, but the toxicity of this schedule was far worse than all the of treatment options. Log tumor growth change per day transformation of the tumor volumes revealed similar tumor growth rates both for flavopiridol then doxorubicin and doxorubicin then flavopiridol combinations, but treatment-related toxicity caused doxorubicin then flavopiridol treatment group to have a significantly different survival than the flavopiridol then doxorubicin–treated animals. H69 exerts different growth kinetics and increased drug resistance *in vivo* (32), and that may be a plausible explanation for the results obtained for H69 cells *in vitro* compared with *in vivo*. The *in vivo* extracellular matrix support might have allowed H69 cells to become less sensitive to flavopiridol and doxorubicin in xenografts and may have somewhat attenuated the response to flavopiridol and doxorubicin combinations from what we expected from the *in vitro* synergism data.

For understanding the role of Rb deficiency in response to flavopiridol and doxorubicin combination, we also used a Rb-positive H865 SCLC model for testing our hypothesis. The caveat is, of course, that each tumor has its own distinct phenotype and consequently sensitivity to doxorubicin varied considerably from one cell type to another. Further, tumor growth rates varied, making comparison of the results of *in vivo* treatment more difficult. Therefore, we followed these studies by knocking down pRb in the H865 cell line to compare this sequence in a cell line that presumably would only differ by the level of pRb expression. The synergistic effect noted with the flavopiridol sequence was coupled with lessened toxicity in these SCLC lines. The H865 cell line was intrinsically more resistant to both flavopiridol and doxorubicin, and knocking down Rb with a specific siRNA vector did not change doxorubicin sensitivity. H865 Rb siRNA clones had a variable amount of Rb expression. The *in vitro* growth kinetics of the H865 Rb siRNA clone was similar to that of H865 parental cell line, but the siRNA Rb clone grew somewhat slower *in vivo*. None of the treatment modalities exerted any *in vivo* tumor growth control for the H865 parental cell line. Doxorubicin alone and doxorubicin then flavopiridol combinations were substantially more toxic than flavopiridol followed by doxorubicin treatment. Seven weeks after one cycle of flavopiridol then doxorubicin treatment, 50% of the animals were still alive. Although this model is very artificial and might not carry the complexities of *de novo* Rb-deficient SCLC, it confirms and extends the observation previously reported for an osteosarcoma cell line and provides a rationale to test sequential low-dose flavopiridol followed by doxorubicin in SCLC and other malignancies that lack functional pRB and are sensitive to doxorubicin.

Low-dose flavopiridol did not exert toxicity but moderately reduced the toxicity of doxorubicin in all of our xenograft models. We did not aim for high-grade cell cycle arrest and apoptosis with flavopiridol-alone treatment (30). With a rather lower dose of flavopiridol, we wanted to induce a relatively longer G_1-S block in normal tissue cells for protection during doxorubicin treatment.

In our experimental model, we used both a *de novo* Rb-deficient SCLC cell line, H69, and a Rb knockdown clone, H865 Rb siRNA clone 12, for evaluating the Rb-dependent effects of flavopiridol and doxorubicin combinations. Rb status in H865 cells did not affect cell growth *in vitro* and had minimally prolonged tumor growth in the H865 Rb siRNA clone 12 model. The cellular response to drug treatments was highly dependent on the Rb status of the cells both *in vitro* and *in vivo*. Flavopiridol then doxorubicin sequential treatment had strong *in vitro* synergism (CI < 0.7) only in Rb-deficient cells, H69, and H865 siRNA clone 12, but was antagonistic in Rb-positive H865 cells. Doxorubicin then flavopiridol treatment had no effect on pRb-negative cells but decreased apoptosis in Rb-positive H865 parental cells in culture. Flavopiridol treatment alone accelerated tumor growth in *de novo* Rb-negative H69 cell line but not in Rb-positive H865 and its Rb knockdown derivative, H865 Rb siRNA clone 12, cells. Additionally, flavopiridol delayed doxorubicin treatment accelerated tumor growth both in Rb-negative and Rb-positive cells. These observations might suggest that tumor growth acceleration occurred in an Rb-independent manner in these models. The flavopiridol then doxorubicin treatment led to increased survival only in Rb-negative xenograft models, H69 and H865 Rb siRNA clone12, by both decreasing toxicity and increasing tumor cell kills.

Downloaded from clincancerres.aacrjournals.org on September 26, 2020. © 2009 American Association for Cancer Research.

Collectively, these results provide evidence that *de novo* Rb status and timing of flavopiridol and doxorubicin combination treatment greatly affects the response. This might have important clinical implications because it suggests that tumor growth could actually be enhanced by the treatment in specific clinical scenarios. The relevance of these observations to the response to this flavopiridol followed by doxorubicin sequence in SCLC patients requires further investigation with clinical trials.

Disclosure of Potential Conflicts of Interest

No potential conflicts of interest were disclosed.

References

1. Govindan R, Page N, Morgensztern D, et al. Changing epidemiology of small-cell lung cancer in the United States over the last 30 years: analysis of the surveillance, epidemiologic, and end results database. J Clin Oncol 2006;24:4539–44.
2. El Maalouf G, Rodier JM, Faivre S, Raymond E. Could we expect to improve survival in small cell lung cancer? Lung Cancer 2007;57 Suppl 2:S30–4.
3. Senderowicz AM. Small-molecule cyclin-dependent kinase modulators. Oncogene 2003;22:6609–20.
4. Thatcher N, Faivre-Finn C, Lorigan P. Management of small-cell lung cancer. Ann Oncol 2005;16 Suppl 2: ii235–9.
5. Ferraldeschi R, Baka S, Jyoti B, Faivre-Finn C, Thatcher N, Lorigan P. Modern management of small-cell lung cancer. Drugs 2007;67:2135–52.
6. Buchholz E, Manegold C, Pilz L, Thatcher N, Drings P. Standard versus dose-intensified chemotherapy with sequential reinfusion of hematopoietic progenitor cells in small cell lung cancer patients with favorable prognosis. J Thorac Oncol 2007;2:51–8.
7. Wistuba II, Gazdar AF, Minna JD. Molecular genetics of small cell lung carcinoma. Semin Oncol 2001;28: 3–13.
8. Wistuba II, Gazdar AF. Characteristic genetic alterations in lung cancer. Methods Mol Med 2003;74: 3–28.
9. Weinberg RA. The retinoblastoma protein and cell cycle control. Cell 1995;81:323–30.
10. Paggi MG, Baldi A, Bonetto F, Giordano A. Retinoblastoma protein family in cell cycle and cancer: a review. J Cell Biochem 1996;62:418–30.
11. Beijersbergen RL, Bernards R. Cell cycle regulation by the retinoblastoma family of growth inhibitory proteins. Biochim Biophys Acta 1996;1287:103–20.
12. Fornari FA, Randolph JK, Yalowich JC, Ritke MK, Gewirtz DA. Interference by doxorubicin with DNA unwinding in MCF-7 breast tumor cells. Mol Pharmacol 1994;45:649–56.
13. Pigram WJ, Fuller W, Hamilton LD. Stereochemistry of intercalation: interaction of daunomycin with DNA. Nat New Biol 1972;235:17–9.
14. Agarwal ML, Taylor WR, Chernov MV, Chernova OB, Stark GR. The p53 network. J Biol Chem 1998;273: 1–4.
15. Muller I, Niethammer D, Bruchelt G. Anthracycline-derived chemotherapeutics in apoptosis and free radical cytotoxicity [review]. Int J Mol Med 1998;1: 491–4.
16. Shapiro GI. Cyclin-dependent kinase pathways as targets for cancer treatment. J Clin Oncol 2006;24: 1770–83.
17. Shapiro GI. Preclinical and clinical development of the cyclin-dependent kinase inhibitor flavopiridol. Clin Cancer Res 2004;10:4270–5s.
18. Sedlacek HH. Mechanisms of action of flavopiridol. Crit Rev Oncol Hematol 2001;38:139–70.
19. Schwartz GK. CDK inhibitors: cell cycle arrest versus apoptosis. Cell Cycle 2002;1:122–3.
20. Zhai S, Senderowicz AM, Sausville EA, Figg WD. Flavopiridol, a novel cyclin-dependent kinase inhibitor, in clinical development. Ann Pharmacother 2002;36: 905–11.
21. Reiner T, de las Pozas A, Perez-Stable C. Sequential combinations of flavopiridol and docetaxel inhibit prostate tumors, induce apoptosis, and decrease angiogenesis in the G-γ/T-15 transgenic mouse model of prostate cancer. Prostate 2006;66:1487–97.
22. Radhakrishnan SK, Gartel AL. A novel transcriptional inhibitor induces apoptosis in tumor cells and exhibits antiangiogenic activity. Cancer Res 2006;66: 3264–70.
23. Newcomb EW. Flavopiridol: pleiotropic biological effects enhance its anti-cancer activity. Anticancer Drugs 2004;15:411–9.
24. Li W, Fan J, Bertino JR. Selective sensitization of retinoblastoma protein-deficient sarcoma cells to doxorubicin by flavopiridol-mediated inhibition of cyclin-dependent kinase 2 kinase activity. Cancer Res 2001;61:2579–82.
25. Semizarov D, Kroeger P, Fesik S. siRNA-mediated gene silencing: a global genome view. Nucleic Acids Res 2004;32:3836–45.
26. Chou TC, Talalay P. Quantitative analysis of dose-effect relationships: the combined effects of multiple drugs or enzyme inhibitors. Adv Enzyme Regul 1984; 22:27–55.
27. Cox DR, Oakes D. Analysis of survival data. New York: CRC Press; 1984.
28. Team RDC. A language and environment for statistical computing. Vienna (Austria): R Foundation for Statistical Computing; 2007.
29. Pinheiro JC, Bates DM. Mixed-effects models in S and S-Plus. New York: Springer-Verlag; 2000.
30. Litz J, Carlson P, Warshamana-Greene GS, Grant S, Krystal GW. Flavopiridol potently induces small cell lung cancer apoptosis during S phase in a manner that involves early mitochondrial dysfunction. Clin Cancer Res 2003;9:4586–94.
31. Bible KC, Kaufmann SH. Flavopiridol: a cytotoxic flavone that induces cell death in noncycling A549 human lung carcinoma cells. Cancer Res 1996;56: 4856–61.
32. Sethi T, Rintoul RC, Moore SM, et al. Extracellular matrix proteins protect small cell lung cancer cells against apoptosis: a mechanism for small cell lung cancer growth and drug resistance *in vivo*. Nat Med 1999;5:662–8.
33. Paik KH, Park YH, Ryoo BY, et al. Prognostic value of immunohistochemical staining of p53, bcl-2, and Ki-67 in small cell lung cancer. J Korean Med Sci 2006; 21:35–9.
34. Breen L, Heenan M, Amberger-Murphy V, Clynes M. Investigation of the role of p53 in chemotherapy resistance of lung cancer cell lines. Anticancer Res 2007;27:1361–4.
35. Alonso M, Tamasdan C, Miller DC, Newcomb EW. Flavopiridol induces apoptosis in glioma cell lines independent of retinoblastoma and p53 tumor suppressor pathway alterations by a caspase-independent pathway. Mol Cancer Ther 2003;2:139–50.
36. Shapiro GI, Koestner DA, Matranga CB, Rollins BJ. Flavopiridol induces cell cycle arrest and p53-independent apoptosis in non-small cell lung cancer cell lines. Clin Cancer Res 1999;5:2925–38.
37. Karp JE, Smith BD, Levis MJ, et al. Sequential flavopiridol, cytosine arabinoside, and mitoxantrone: a phase II trial in adults with poor-risk acute myelogenous leukemia. Clin Cancer Res 2007;13:4467–73.
38. Motwani M, Rizzo C, Sirotnak F, She Y, Schwartz GK. Flavopiridol enhances the effect of docetaxel *in vitro* and *in vivo* in human gastric cancer cells. Mol Cancer Ther 2003;2:549–55.
39. Schwartz GK, O'Reilly E, Ilson D, et al. Phase I study of the cyclin-dependent kinase inhibitor flavopiridol in combination with paclitaxel in patients with advanced solid tumors. J Clin Oncol 2002;20:2157–70.
40. Shah MA, Kortmansky J, Motwani M, et al. A phase I clinical trial of the sequential combination of irinotecan followed by flavopiridol. Clin Cancer Res 2005;11: 3836–45.
41. Gomez LA, de Las Pozas A, Perez-Stable C. Sequential combination of flavopiridol and docetaxel reduces the levels of X-linked inhibitor of apoptosis and AKT proteins and stimulates apoptosis in human LNCaP prostate cancer cells. Mol Cancer Ther 2006; 5:1216–26.
42. Wittmann S, Bali P, Donapaty S, et al. Flavopiridol down-regulates antiapoptotic proteins and sensitizes human breast cancer cells to epothilone B-induced apoptosis. Cancer Res 2003;63:93–9.
43. Mihara M, Shintani S, Nakashiro K, Hamakawa H. Flavopiridol, a cyclin dependent kinase (CDK) inhibitor, induces apoptosis by regulating Bcl-x in oral cancer cells. Oral Oncol 2003;39:49–55.
44. Mayer F, Mueller S, Malenke E, Kuczyk M, Hartmann JT, Bokemeyer C. Induction of apoptosis by flavopiridol unrelated to cell cycle arrest in germ cell tumour derived cell lines. Invest New Drugs 2005;23: 205–11.
45. Ma Y, Cress WD, Haura EB. Flavopiridol-induced apoptosis is mediated through up-regulation of E2F1 and repression of Mcl-1. Mol Cancer Ther 2003;2:73–81.
46. Li Y, Chinni SR, Senderowicz AM, Sarkar FH. Induction of growth inhibition and apoptosis in prostate cancer cells by flavopiridol. Int J Oncol 2000;17: 755–9.
47. Kitada S, Zapata JM, Andreeff M, Reed JC. Protein kinase inhibitors flavopiridol and 7-hydroxystaurosporine down-regulate antiapoptosis proteins in B-cell chronic lymphocytic leukemia. Blood 2000; 96:393–7.
48. Brueckl WM, Herbst L, Lechler A, et al. Predictive and prognostic factors in small cell lung carcinoma (SCLC)—analysis from routine clinical practice. Anticancer Res 2006;26:4825–32.
49. Charpidou A, Hatzidarellis EP, Alamara C, et al. Pegylated liposomal doxorubicin HCL (Caelyx) in combination with sandostatin LAR as salvage therapy in patients with small-cell lung cancer. In Vivo 2006; 20:553–7.
50. Cheng S, Evans WK, Stys-Norman D, Shepherd FA. Chemotherapy for relapsed small cell lung cancer: a systematic review and practice guideline. J Thorac Oncol 2007;2:348–54.

Downloaded from clincancerres.aacrjournals.org on September 26, 2020. © 2009 American Association for Cancer Research.

AACR American Association for Cancer Research

Clinical Cancer Research

Retinoblastoma Tumor Suppressor Gene Expression Determines the Response to Sequential Flavopiridol and Doxorubicin Treatment in Small-Cell Lung Carcinoma

Tulin Budak-Alpdogan, Bobin Chen, Anjali Warrier, et al.

Clin Cancer Res 2009;15:1232-1240.

Updated version	Access the most recent version of this article at: http://clincancerres.aacrjournals.org/content/15/4/1232
Supplementary Material	Access the most recent supplemental material at: http://clincancerres.aacrjournals.org/content/suppl/2009/02/16/1078-0432.CCR-08-0810.DC1

Cited articles	This article cites 47 articles, 21 of which you can access for free at: http://clincancerres.aacrjournals.org/content/15/4/1232.full#ref-list-1
Citing articles	This article has been cited by 1 HighWire-hosted articles. Access the articles at: http://clincancerres.aacrjournals.org/content/15/4/1232.full#related-urls

E-mail alerts	Sign up to receive free email-alerts related to this article or journal.
Reprints and Subscriptions	To order reprints of this article or to subscribe to the journal, contact the AACR Publications Department at pubs@aacr.org.
Permissions	To request permission to re-use all or part of this article, use this link http://clincancerres.aacrjournals.org/content/15/4/1232. Click on "Request Permissions" which will take you to the Copyright Clearance Center's (CCC) Rightslink site.

Downloaded from clincancerres.aacrjournals.org on September 26, 2020. © 2009 American Association for Cancer Research.